

## Research Article

# IEEE 802.11-Based Wireless Sensor System for Vibration Measurement

Yutaka Uchimura,<sup>1</sup> Tadashi Nasu,<sup>2</sup> and Motoichi Takahashi<sup>2</sup>

<sup>1</sup> Shibaura Institute of Technology, 3-7-5 Toyosu, Koto-ku, Tokyo 135-8548, Japan

<sup>2</sup> Kajima Corporation, 1-3-1 Motoakasaka, minato-ku, Tokyo 107-0051, Japan

Correspondence should be addressed to Yutaka Uchimura, uchimura@sic.shibaura-it.ac.jp

Received 15 October 2009; Revised 17 December 2009; Accepted 15 January 2010

Academic Editor: Yi Qing Ni

Copyright © 2010 Yutaka Uchimura et al. This is an open access article distributed under the Creative Commons Attribution License, which permits unrestricted use, distribution, and reproduction in any medium, provided the original work is properly cited.

Network-based wireless sensing has become an important area of research and various new applications for remote sensing are expected to emerge. One of the promising applications is structural health monitoring of building or civil engineering structure and it often requires vibration measurement. For the vibration measurement via wireless network, time synchronization is indispensable. In this paper, we introduce a newly developed time synchronized wireless sensor network system. The system employs IEEE 802.11 standard-based TSF-counter and sends the measured data with the counter value. TSF based synchronization enables consistency on common clock among different wireless nodes. We consider the scale effect on synchronization accuracy and evaluated the effect by taking beacon collisions into account. The scalability issue by numerical simulations is also studied. This paper also introduces a newly developed wireless sensing system and the hardware and software specifications are introduced. The experiments were conducted in a reinforced concrete building to evaluate synchronization accuracy. The developed system was also applied for a vibration measurement of a 22-story steel structured high rise building. The experimental results showed that the system performed more than sufficiently.

## 1. Introduction

Rapid progress of wireless network technology and embedded sensor technology has been integrated into wireless sensor network and various prospective applications are expected to emerge. Among the many sensing network applications, particularly promising one is the structure health monitoring, which monitors the structural health of buildings and civil engineering structures [1]. Since measuring objects such as a bridge and a building are usually huge and installing very long signal cables requires high installation cost. Additionally, long cables leave wires vulnerable to ambient signal noise corruption, thus wireless data transmission is highly beneficial. Structure health monitoring often requires measuring vibration data such as acceleration and velocity. Measured data are analyzed by the modal analysis method to obtain the resonance frequency, damping ratio and spectrum response [2].

For wireless vibration measurements, time synchronization is very important because the vibration measurement for the modal analysis requires simultaneous multipoint sensing data which are often transmitted via multihop relayed wireless devices. Due to the queuing process and stochastic media access method, the data transmissions are randomly delayed. As a result, even if each sensor node acquires data and sends them exactly at the same instant, the arrival time of the data does not match. To avoid it, the received data needs to be adjusted so as to maintain the time consistency on a common time axis. Because when the data are used for modal analysis, a time difference may be misunderstood as a phase shift. To maintain precise time consistency among wireless nodes, time synchronization is indispensable.

In this paper we propose a synchronization method for wireless sensor network system, which utilizes IEEE 802.11-based timing synchronization function (TSF). The function

is a mechanism for synchronizing local timer counter of each wireless device, which is originally used for contention control among wireless node. By embedding the value of TSF counter in a packet with measured data, one can solve the time skew problem on the receiver side.

In the following section, we briefly review the related works. Section 3 describes the adverse effects on vibration sensing caused by a time delay in wireless network and denotes the reason why time synchronization is needed. Section 4 describes a probability of timing synchronization beacon transmission. The section also describes stochastic analysis and simulation studies on the scalability of sensor network. In Section 5, we describe a newly developed wireless sensing system and also describe its hardware and software components. In Section 6, experimental evaluations of time synchronization accuracy and vibration measurement data in a high rise building are presented.

## 2. Related Works

Time synchronization of network is indispensable to manage transmission timing and to avoid wasteful collisions, therefore several technologies such as GPS, radio ranging have been used to provide global synchronization in networks. GPS-based synchronization offers very precise synchronization, however it is not always available indoor place [3]. In wired network, the Network Time Protocol (NTP) has been developed that has kept the Internet's clocks ticking in phase [4].

RT-Link [5] uses media access control (MAC) based on slotted ALOHA and it employs independent AM carrier-current radio device for indoor time synchronization. However, carrier-current AM is only allowed on the school campus in the United States, so long as the normal FCC Part 15. [6] Berkeley MAC (B-MAC) supports carrier sense multiple access (CSMA) with low power listening where each node periodically wakes up after a sample interval and checks the channel for activity for a short duration. The main concern of these methods is battery life, because time synchronization is one of the most important factors to determine radioactive period, which directly affects battery life. There have been many studies on time synchronization which mainly aimed for conserving battery energy of network nodes.

Meanwhile, IEEE 802.11 [7] standard devices have a timing synchronization function (TSF) by default. We propose to utilize the function for synchronization among nodes to determine the sampling data interval and the time stamping of measured data. IEEE 802.11 is one of the de facto standards of the wireless local area network and so is easily obtained with industrial-level reliability. Furthermore, the modulation employs Direct Sequence Spread Spectrum (DS-SS) and Orthogonal Frequency Division Multiplexing (OFDM) which offer robustness against phasing and noise. Those are advantages against RT-Link and Berkeley Mote which use noise susceptible wireless modulation.

Some studies pointed out the scalability issue on IEEE 802.11 TSF [8] and new protocols such as SATSF [9] and MATSF [10] were proposed to achieve very accurate clock synchronization; however they are still on the research

level and not implemented on market ready products. Even though the current 802.11 TSF is involved with the scalable issue, it depends on the scale and the requirement of accuracy of the application. Our targeted application uses less than 100 nodes and required accuracy is around 1 to 10 milliseconds. Additionally, thanks to the progress of the wireless technology, the synchronization error rates are decreased and consequently accuracy is improved comparing to the results shown in [8].

We made simulation-based analyses and verified that even the original 802.11 TSF is accurate enough for vibration measurement.

## 3. Time Delay on Wireless Network

The data transmission via a wireless network requires certain amount of time elapsing from the moment when the transmitter sends the data to the moment when the data arrives at the receiver. In the building vibration measurement applications, sensors usually need to be placed at several points on different floors in a building. A measurement station (host computer) is placed at a certain location in the building. In such cases, especially in a high rise building, the wireless radio waves of each sensor node do not directly reach the station. Thus, the multihop network path is required and the packets are transmitted in relays of the wireless sensor nodes.

Therefore, even if all the nodes intend to send packets at exactly the same time, the arrival times may be different. This fact results serious problem when measured data are used for modal analysis, because time delay may cause unexpected fake mode. Therefore we somehow need to maintain consistency of received data on the common time axis.

To resolve this issue, we propose to send the vibration data together with the time stamp at the moment when the data is measured. After the data are received at the host PC, they can be rearranged along the common time axis based on the time stamp. This procedure is valid provided that all clocks of the nodes are matched. However, accuracy of the quartz crystal oscillator is affected by many factors such as temperature and change of current or voltage [11]. Frequency stability of oscillators used for PCs is mostly around  $10^{-4}$  (100 ppm). Imprecision of 100 ppm corresponds to a 1 millisecond (10 msec) error in 10 seconds, or an 18-degree phase error for 100 Hz vibration. Even though the resonant frequency of a building is low (typically less than 10 Hz), a 1 msec difference between the fastest clock and the slowest clock is more than negligible amount. Therefore, periodical time synchronization is indispensable and accuracy of the synchronization is the matter of concern.

## 4. Synchronization Issue on Scalability

*4.1. IEEE 802.11-Based TSF Mechanism and Contention Process.* The accuracy of the synchronization is one of the most concerning issues in wireless sensor networks. As described in the previous section, we use IEEE 802.11-based TSF. IEEE 802.11 based TSF synchronizes the clock

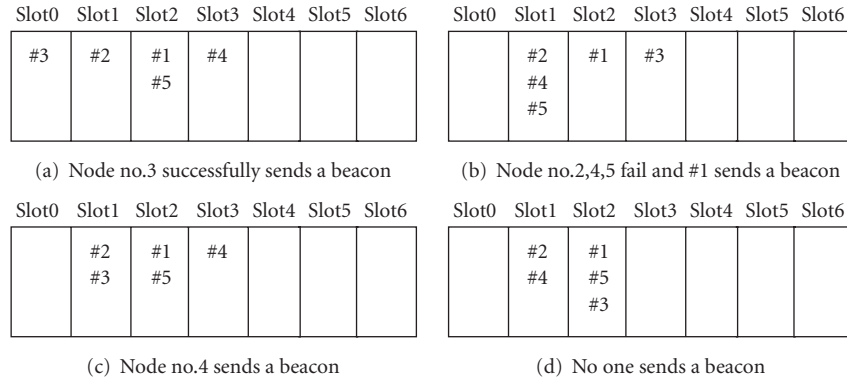


FIGURE 1: Slot allocation and transmission contention.

in stochastic manner, that is, the synchronization contains random factors. As a result, the accuracy can only be evaluated by probability analysis. Before describing the detail of the analysis, we briefly describe the mechanism of TSF.

Suppose there are several nodes within the radio range, which can communicate each other and they form independent basic service set (IBSS). Each node ticks its own TSF counter (64 bit) by 1 nanosecond. The nodes in the IBSS contend a right to send a beacon and one or more nodes becomes eligible to send a beacon. In each beacon transmission period, several slots are prepared and each node is randomly assigned into a certain slot as shown in Figure 1, where no. 1 or no. 2 denotes the number of node. Each slot may hold none or one or more nodes. In the beginning of each beacon transmission period, the nodes in the least slot number send a beacon which contains TSF counter value. If there exist only one node in the slot, the beacon packet is successfully sent (Figure 1(a)) and the other node adjust their TSF counter only if the received value of the TSF counter is larger than the received value. If the received value is smaller, the nodes do not adjust own counter.

On the other hand, if there are two or more nodes in the same slot as shown in Figure 1(b), they start transmitting a beacon packet in the same time, thus the beacon packets collide and transmission results to fail. If it fails, the nodes in the second least slot number transmit a beacon. In Figure 1(b) case, node #1 sends a beacon without collision. These sequences are repeated as long as available slots remain. It may happen that no successful beacon transmission during the beacon period as shown in Figure 1(d), they need to wait for next beacon period (typically 100 milli-seconds later).

In Figure 1 case, we suppose 5 nodes and 7 slot spaces; however one may easily imagine that the chance of successful beacon transmission decreases if the number of nodes increases, while the number of slots is limited. The successful rate depends on the number of nodes and slots. Because the slot allocation is randomly determined, analysis based on probability theory is required.

Huang and Lia [8] pointed out the issue and showed analyses and simulation results on the synchronization error. The paper offered great contribution for the probabilistic analysis; however the specification of the device is obsolete.

For example, the bit-rate in the simulation is fixed to 1 Mbps because it was the maximum speed at that time.

In order to match up to current technology and give a prospective aspect of 802.11-based time synchronization, we made analysis on scalability effect of IEEE 802.11 a/b/g standard based sensor stations. In the followings, we describe the probability theory-based formulas of success rate of the beacon transmission. Then we show results of the numerical analysis in case of various bit rates, modulations and number of wireless stations.

*4.2. Probability of Successful Beacon Transmission.* In IEEE 802.11 standards, the number of the slots is  $2 \cdot \text{aCWmin} + 1$  and each node is scheduled to transmit a beacon at the beginning of one of the slots, where aCWmin is the minimum contention window for the media. The value of aCWmin is 31 in Direct Sequence Spread Spectrum (DSSS) and 15 in Orthogonal Frequency Division Multiplexing (OFDM).

Let us suppose the length of a beacon is  $L_b$  (bit), the transmission bit rate is  $T_r$  (Mbps) and the time length of a slot time is  $S_t$  ( $\mu$ sec), the integer number of slots occupied by a beacon ( $N_s$ ) is obtained in (1),

$$\frac{L_b}{T_r S_t} \leq N_s \leq \frac{L_b}{T_r S_t} + 1, \quad (1)$$

where  $N_s$  can be also obtained by roundup function of  $L_b/T_r S_t$ .

Once a beacon transmission starts, other nodes need to be quiet for the time length of  $N_s$  slots. If a beacon transmission fails, they resume counting down the back-off timer and contending for the remaining slots. If the collisions occur by  $m$  times in series and all available slots are consumed, that is, corresponds the condition in (2) becomes true, the beacon transmission trials fell through

$$2 \cdot \text{CWmin} + 1 - m \cdot N_s \leq 0. \quad (2)$$

As stated above, the beacon transmission is not deterministic, thus we need to analyze it by stochastic manner.

First of all, let us reconfirm the definition of successful beacon transmission. We define that a beacon is transmitted

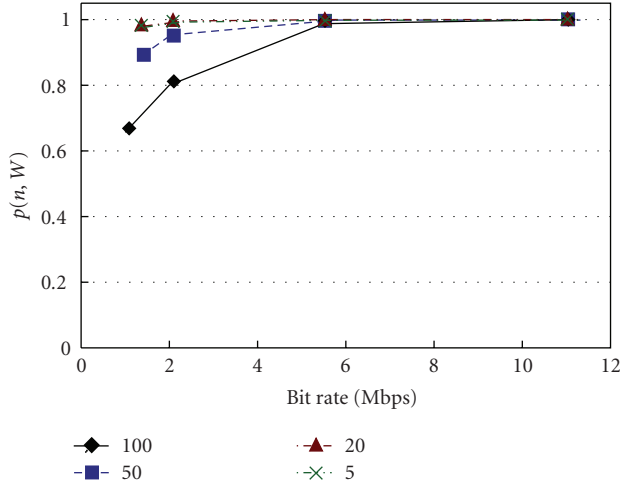


FIGURE 2: Successful beacon transmission rate of 802.11b.

TABLE 1: Specifications of 802.11a/b/g.

	aCWmin	Bit Rate (Mbps) (min-max)	Slot Time ( $\mu$ sec)
802.11a	15	6-54	9
802.11b	31	1-11	20
802.11g	15	6-54	9/20

successfully if at least one node transmits a beacon successfully during a beacon transmission period. Suppose that the IBSS consists of  $n$  nodes and let  $W$  be twice the minimum contention window ( $W = 2 \cdot \text{aCWmin}$ ). Let  $p(n, W)$  be the probability that at least one of the  $n$  nodes succeeds in a beacon transmission, then  $p(n, W)$  is given by the recursive formula shown in (3):

$$p(n, W) = \left(\frac{W}{W+1}\right)^n p(n, W-1) + n \left(\frac{1}{W+1}\right) \left(\frac{W}{W+1}\right)^{n-1} + q(n, W). \quad (3)$$

The first term corresponds to the probability of the event that there is no beacon transmission in slot 0, while there is a successful beacon transmission in window  $[1, W]$ . The second term corresponds that there is a successful beacon transmission in slot 0. The third term  $q(n, W)$  is the probability that there is unsuccessful transmission in slot 0, but at least one beacon transmission in window  $[1, W]$ . The formula for  $q(n, W)$  is shown in (4):

$$q(n, W) = \sum_{i=2}^n \sum_j^{n-i} \left\{ C_i^n C_j^{n-i} \left(\frac{W}{W+1}\right)^i \left(\frac{N_s-1}{W+1}\right)^j \left(\frac{W-N_s+1}{W+1}\right)^{n-i-j} p(n-i-j, W-N_s) \right\}, \quad (4)$$

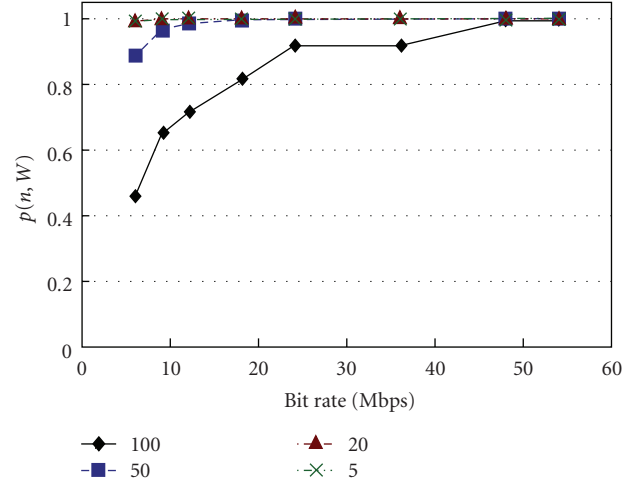


FIGURE 3: Successful beacon transmission rate of 802.11g (20 microsec).

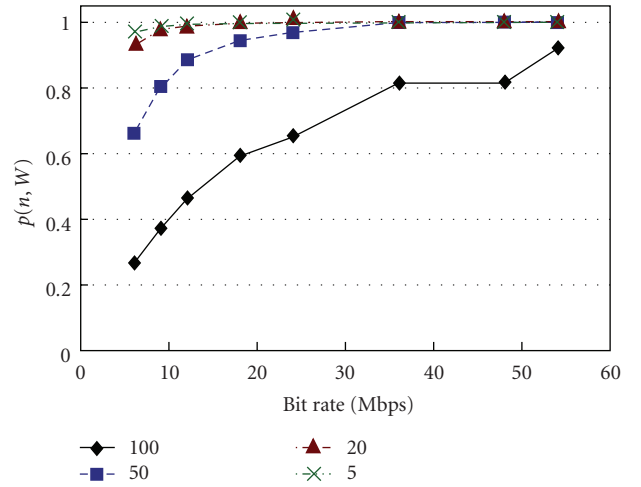


FIGURE 4: Successful beacon transmission rate of 802.11a/ pure g (9 microsec).

where  $C_k^n$  is the combination number defined in (5):

$$C_k^n = n(n-1) \cdots \frac{n-k+1}{k!}. \quad (5)$$

**4.3. Numerical Analysis on Probability of Beacon Transmissions.** Based on the formulas shown in (3) and (4) the probability can be calculated for given  $n$ ,  $W$ , and  $N_s$ . Notice that  $W$  has a different value depending on the modulation type, which is 63 in DSSS and 30 in OFDM. In IEEE std. based wireless network, 802.11a and 802.11g use OFDM and 802.11b uses DSSS.

$N_s$  defined in (1) is determined based on bit rate  $T_r$  (bps), the length of a beacon  $L_b$  (bit) and slot time  $S_t$  ( $\mu$ sec). Values of these parameters and their ranges are shown in Table 1.

The slot time for 802.11g is 20 ( $\mu$ sec) when there is 802.11b node within the radio range, while the slot time of

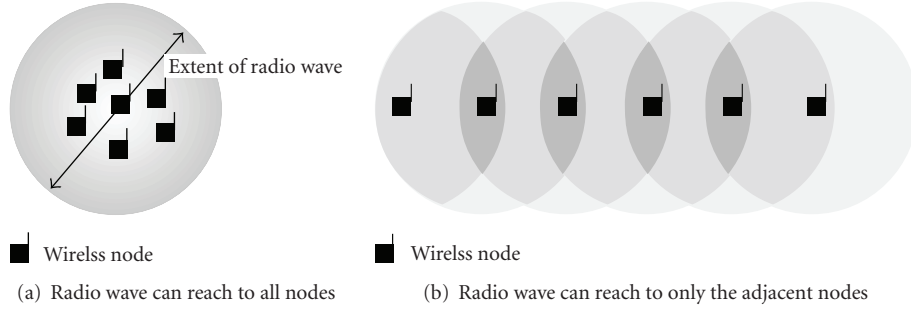
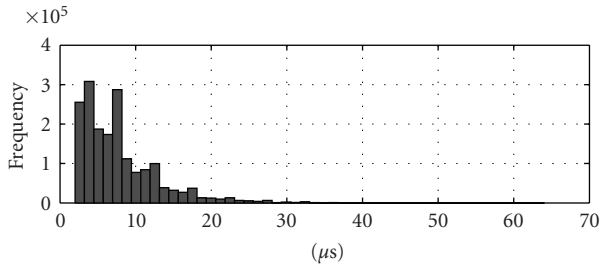
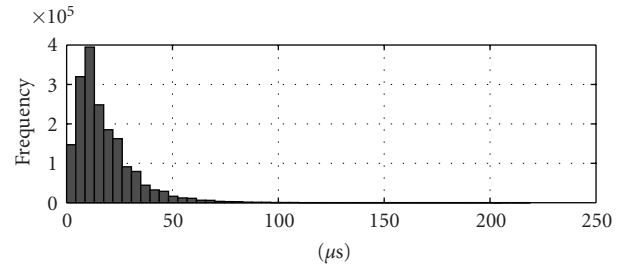


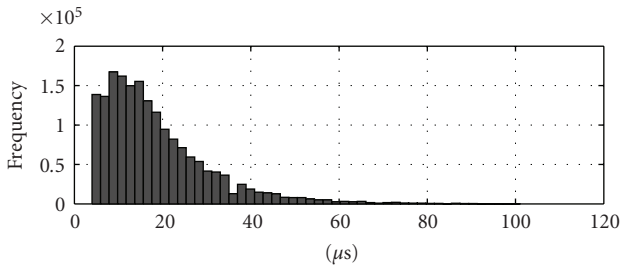
FIGURE 5: Configuration of wireless nodes.



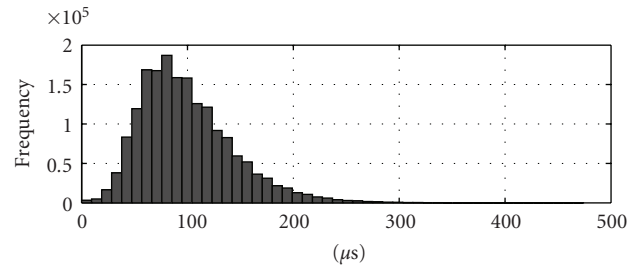
(a) Case 1: Maximum Offset in 5 nodes (microsec)



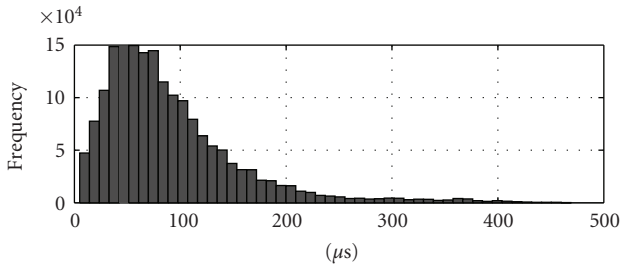
(a) Case 2: Maximum Offset in 5 nodes (microsec)



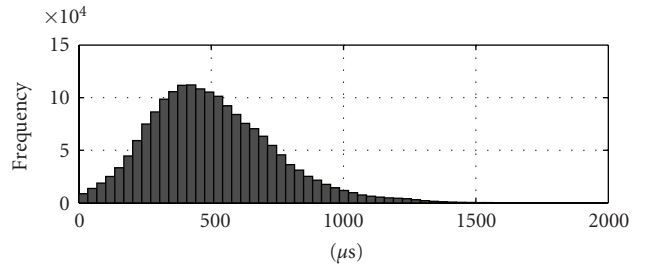
(b) Case 1: Maximum Offset in 20 nodes (microsec)



(b) Case 2: Maximum Offset in 20 nodes (microsec)



(c) Case 1: Maximum Offset in 100 nodes (microsec)



(c) Case 2: Maximum Offset in 100 nodes (microsec)

FIGURE 6: Histogram of the maximum offset value in Case 1.

FIGURE 7: Histogram of the maximum offset value in Case 2.

a pure 802.11g network is 9 ( $\mu\text{sec}$ ). Length of a beacon depends on the size of contained information. For example, length of the service set ID is between 2 and 34 bytes, the length of supported rates and the extended supported rate are also variable. In the simulation, we assumed the length of a beacon is 110 bytes which is the real beacon size of a prototype system.

Substituting (4) into (3) gives recursive equation of  $p(n, W)$ . Using the boundary condition  $p(0, W) = p(n, 0) = 0$ ,  $p(n, W)$  is calculated for given  $N_s$ .

Figures 2, 3, and 4 shows the results of calculation of the probability rate of successful beacon transmission  $p(n, W)$ . The horizontal axis is bit rates and each plot line shows the case of different number of nodes.

Figure 2 is the result of 802.11b. Figure 3 is the result of 802.11g with 20  $\mu\text{sec}$  slot time and Figure 4 is the result of 802.11 a/g with 9  $\mu\text{sec}$ . As shown in three graphs, the rates increase in larger bit rates. On the other hand, the rate decreases with growth of number of nodes. Another aspect of the results shows that the short slot time deteriorates

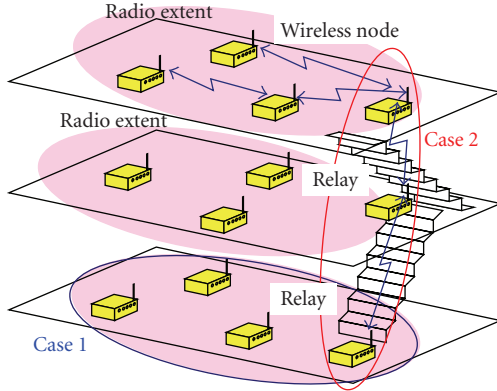


FIGURE 8: Measurement configuration in a building as mixture of Cases 1 and 2.

the beacon successful rate  $p(n, W)$ , which is observed in comparison of Figures 3 and 5 (802.11g with short slot time). This is because number of occupied slots increases for shorter slot time or low bit rate, and chance of beacon transmission become smaller.

In the case of 802.11a/g with  $9 \mu\text{sec}$ ,  $p(n, W)$  drops down to 0.26 for 100 nodes, which is the minimum rates among the results. Considering these results, we made numerical simulations to evaluate the synchronization accuracy.

**4.4. Simulations on Synchronization Accuracy.** In the TSF-based synchronization, a node which receives a beacon adjusts its TSF counter to the time stamp of the received beacon if the value of the time stamp is later than the node's TSF counter. (It is important to note that clocks only move forward and never backward). Possibility of chance to send a beacon is equal, thus the node whose clock is fastest seldom gain a chance to adjust one's clock to others. As a result, the offset of TSF (the deference of TSF counter between the fastest node and the slowest node) becomes large as the number of nodes in the IBSS grows.

The offset of TSF also strongly depends on the configuration of nodes in the segment. Therefore we classified them into two configuration cases.

**Case 1.** All nodes exist within the range that radio waves can reach (Figure 5(a)), that is, each node can send a beacon directly to any other nodes.

**Case 2.** All nodes are arranged so that radio waves can reach two adjacent nodes only (right and left nodes). Figure 5(b) illustrates the allocation of nodes. End-to-end communication is possible only through multihop relays.

Numerical simulations were set up for the two configuration cases. In addition, the probability of beacon transmission which is analyzed in the previous subsection is taken into account in Case 1, while it is not in Case 2. Because a beacon transmission is contended with only adjacent nodes in Case 2, the beacon transmission rate is always almost 100%.

TABLE 2: Hardware specifications of a wireless node.

	Specification
CPU	CPU Geode GX1 300 MHz
Chip set	NS Geode 5530A
Motherboard	3.5-inch SBC/NS
RAM	SODIMM 256 MB
External Storage	Compact Flash
Extension Bus	PC104
Wireless LAN	NEC WL54AG
Wireless Chip	Atheros 5001X
A/D Converter	16CH, 16 bit Resolution

We run the simulations assuming that TSF clock frequencies were uniformly distributed in the range of  $\pm 50$  ppm ( $\pm 5.0 \times 10^{-5}$ ) and the beacon interval was assumed to be 100 msec. Each simulation trial was conducted for corresponding to 180 seconds elapse of time. In each trial, the TSF clock speed of each node was randomly selected and the total number of trials was 1000 times, which was large enough for data convergence. During the simulation, we recorded the maximum offset which corresponds to the difference between the fastest clock and the slowest clock at each beacon interval. (Notice that the slowest clock does not indicate a clock of specified node.)

Figure 6 shows the results of Case 1 simulation of pure 11g (or 802.11a) with 6 Mbps which is least successful rate of transmission. Figure 6(a) is the case when the total number of nodes is 5 with successful rate 0.969, Figure 6(b) is the case of 20 nodes with successful rate 0.924 and Figure 6(c) is the case of 100 nodes with successful rate 0.262, cf.  $p(n, W)$  in Figure 4.

As shown in the figures, the accuracy of time synchronization gets worse as the number of nodes increases. In 5-node case, 99.9% of the data maintained less than  $36 \mu\text{sec}$ ,  $87 \mu\text{sec}$  in 20-node, and  $428 \mu\text{sec}$  in 100-node case. The median value of 5-node was  $6 \mu\text{sec}$ , that of 20-node case is  $15 \mu\text{sec}$  and  $75 \mu\text{sec}$  in 100 case.

Figure 7 shows the results of Case 2. Figure 7(a) is the case of 5 nodes; Figure 7(b) is that of 20 nodes and Figure 7(c) shows 100-node case. The median value in 5-node case was  $14 \mu\text{sec}$ ,  $92 \mu\text{sec}$  in 20-node case, and  $475 \mu\text{sec}$  in 100-node case. In 5-node case, 99.9% of the data maintained less than  $104 \mu\text{sec}$ ,  $303 \mu\text{sec}$  in 20-node, and  $1388 \mu\text{sec}$  in 100-node case.

Comparing the results of Cases 1 and 2, daisy chain configuration like Case 2 is inferior in synchronization accuracy even though the beacon successful rate is less than 30%.

In vibration measurement for a building or a civil structure, wireless device allocation is likely to be a mixture of Cases 1 and 2. As illustrated in Figure 8, several wireless nodes are located on the same floor and one of them relays packets to the nodes on a different floor. The relay nodes (Case 2) are located in the staircase area. Because the radio power is much attenuated when passing a reinforced concrete

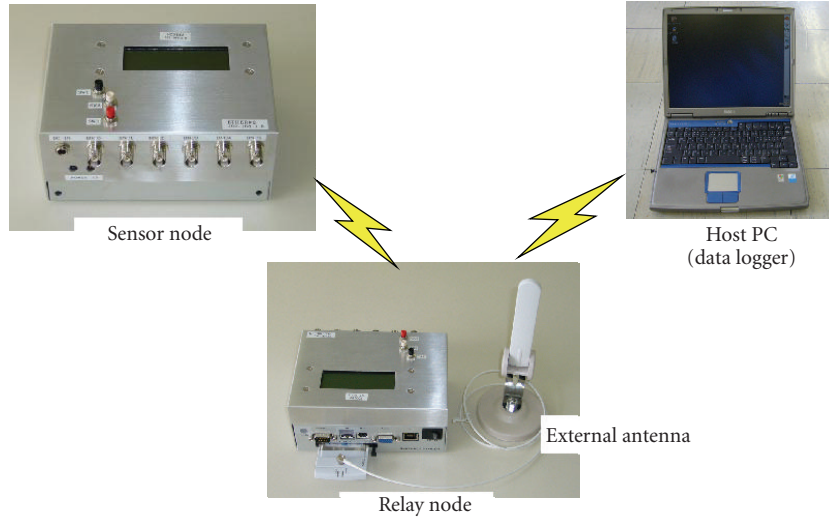


FIGURE 9: Basic components of the developed vibration measurement system.



FIGURE 10: Reinforced concrete building where experiment were conducted.

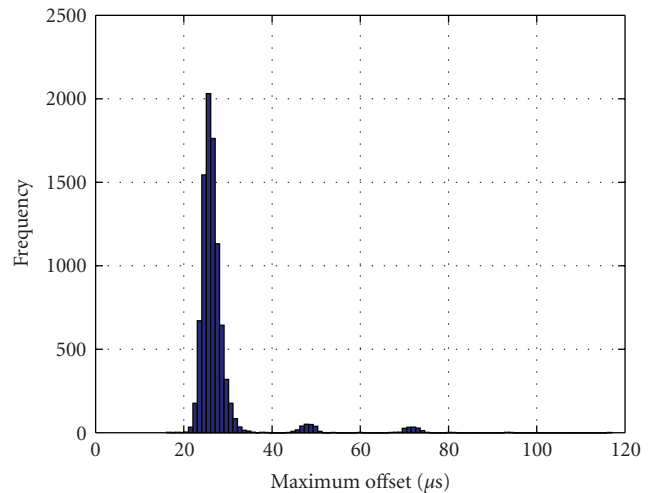


FIGURE 12: Maximum clock offset with three wireless nodes.

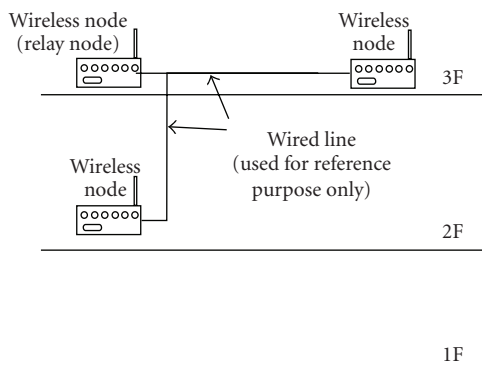


FIGURE 11: Allocation of wireless node.

floor, thus nodes in the different floor can communicate only via Case 2 relay nodes.

The target synchronization accuracy is to maintain within 1 msec. From the simulation results, synchronization accuracy was maintained even when the total number of nodes less than 100 nodes.

### 5. Development of Wireless Measurement System

We developed a wireless embedded measurement system which can be applicable for vibration measurement. Figure 9 is a photo of basic components of the vibration measurement system which consists of a sensor node, a relay node and a host PC. The sensor node and relay node have identical architecture. Size of a node device is 120×70×50 (mm). Main components and their functions of the wireless node are briefly shown in Table 2. The A/D converter has 16CH single end input and 6CH of them are supplied via the BNC jacks. The sampling rate of A/D depends on the measurement object. In the building measurement case, it is at most 100 Hz. It is for conducting the over sampling with digital filters, even though the resonance frequency of a building is less than 10 Hz. The power consumption of a node is typically 7.5 W.

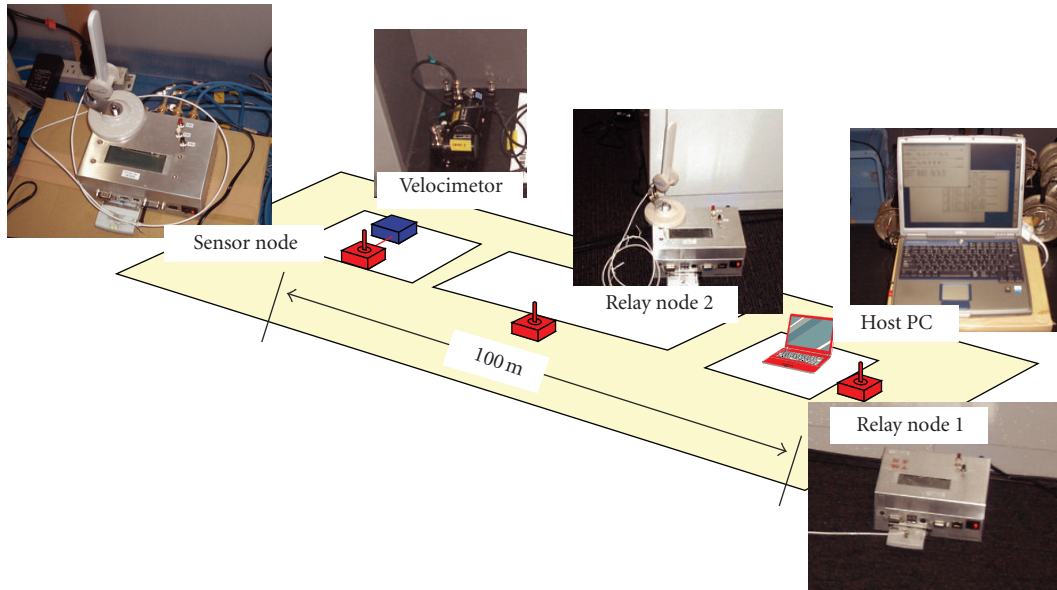


FIGURE 13: Allocation and photos of sensor node, relay node and Host PC.

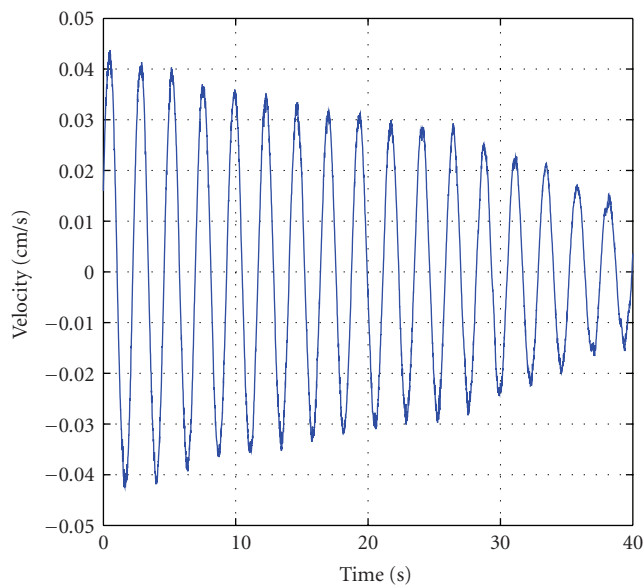


FIGURE 14: Measurement result by the developed wireless system.

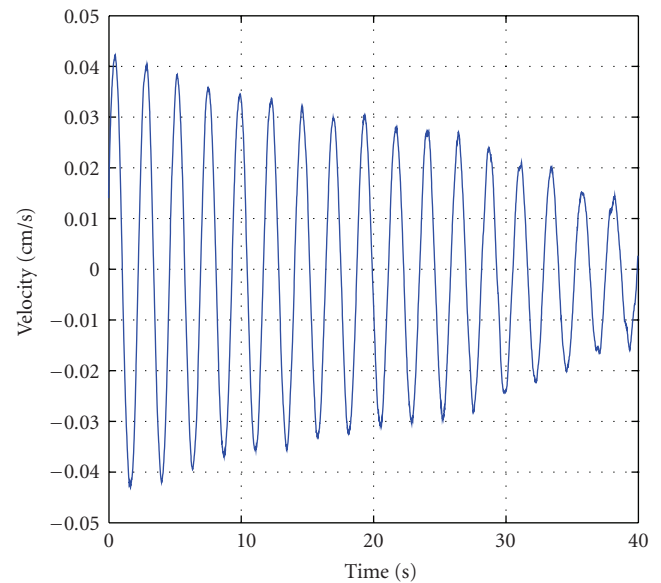


FIGURE 15: Measurement result by the conventional wired data logger.

In this system, sensors are not embedded within it. Because the vibration sensing uses various sensors such as accelerometers or velocity sensors depending on the structure of the buildings, separation of sensor, and wireless node makes it more versatile.

The operating system (OS) for a wireless node is RT-Linux, which is an extension of Linux to a real-time operating system. Software including OS is implemented in a flash memory and the memory can also store measured data. For a wireless device we used IEEE 802.11a/b/g standard wireless network interface card to which an external antenna can be connected.

## 6. Experimental Evaluation of Synchronization Accuracy

*6.1. Experimental Evaluation of Synchronization Accuracy.* For the purpose of evaluating TSF-based synchronization, we made experiments in a three-story reinforced concrete building (Figure 10). As well known, the wireless transmission may not go through the reinforced concrete because the mesh of rebar shields the radio waves. Therefore relay nodes are indispensable. The allocation of wireless node is depicted in Figure 11. We used three wireless nodes which were arranged to make two-hop transmission, that is,

the end-to-end communication packets were relayed via the relay node. Wired signal lines were connected to all nodes for the reference purpose and rectangular wave voltage was supplied on the lines to generate hardware interrupt. Every moment when the voltage of square wave rose, an interrupt occurred exactly at the same moment in three wireless nodes. And TSF count was recorded in the hardware interrupt handler routine.

We evaluated the synchronization accuracy by comparing recorded TSF counter of three nodes. The frequency of square wave was set to 10 Hz, that is, the TSF counter value was recorded every 100 msec. One measurement was continued for 15 minutes thus total number of TSF record sets was 9,000. After the measurement, the maximum offset between recorded set was calculated. We made totally 15 times of 15-minute measurements, thus total number of samples were 135,000.

Figure 12 shows the result of the maximum offset of TSF count, which corresponds to synchronization accuracy. As shown the figure, the median value was 27  $\mu$ sec. The result is close to the simulation result of Case 2 in 5 nodes. The simulation analysis did not take account for any processing time and bit error rate. Therefore, the experimental results must be more realistic when implementing on a real hardware. Nevertheless, the result shows sufficiently accurate synchronization and it maintained good enough accuracy against targeted 1 msec accuracy.

**6.2. Vibration Measurement in a High Rise Building.** We also conducted experimental measurements by using the developed wireless system. The vibration measurement was taken placed in a steel structured 22-story building. Figure 13 shows the allocation of the sensor node, relay nodes and host PC in the measurement room. A velocimeter (velocity sensor) on 22th floor is connected to the measurement node by a coaxial signal cable. The distance between the sensor node and the host PC was about 100 m and the path includes areas partitioned by a steel door and some over-the horizon corners. Thus, we allocated two relay nodes for hooking up the ad-hoc network.

The velocity data was also recorded with conventional wired measurement. Figure 14 shows the measured data of the developed wireless system and Figure 15 shows the data of the conventional wired data logger. The data are damped vibration wave obtained during the forced shaking test. When comparing these two results, the response near the peak of sinusoidal wave is a little bit jaggy in Figure 14 while it is smooth in Figure 15. This is because the difference of the cut-off frequency of the low pass-filters. Except that the data plot almost exactly match. The resonant frequency obtained from both data was 0.425 (Hz) and damping ratio was 0.672 (%). These two values obtained by both methods (wired/wireless) were also matched up to three significant figures.

## 7. Conclusion

For the vibration measurement via wireless network, time synchronization is indispensable. In this paper, we proposed

a new time synchronized wireless sensor network system which employed IEEE 802.11 standard-based TSF counter. It ensured consistency on the common clock among different wireless nodes. The scale effect on the accuracy when the size of nodes increased was evaluated by simulation studies and the result outlined the size which maintains the offset within 1msec. We also described a newly developed wireless sensing system and showed experimental evaluations, which were conducted in a reinforced concrete building. The system was also applied for the vibration measurement of a 22-story steel structured high rise building. The experimental results showed good performance enough for vibration measurement purpose.

## References

- [1] J. P. Lynch, et al., "Post-seismic damage assessment of steel structures instrumented with self-interrogating wireless sensors," in *Proceedings of the 8th National Conference on Earthquake Engineering*, pp. 18–22, 2006.
- [2] Y. Wang, et al., "Vibration monitoring of the voigt bridge using wired and wireless monitoring systems," in *Proceedings of the 4th China-Japan-US Symposium on Structural Control and Monitoring*, 2006.
- [3] H. El Natour, et al., "Analysis of the GPS acquisition environment: indoors and outdoors," in *Proceedings of the 2nd International Conference on Information and Communication Technologies*, vol. 1, pp. 127–132, 2006.
- [4] D. L. Mills, "Internet time synchronization: the network time protocol," in *Global States and Time in Distributed Systems*, IEEE Computer Society Press, New York, NY, USA, 1994.
- [5] A. Rowe, R. Mangharam, and R. Rajkumar, "RT-Link: a time-synchronized link protocol for energy-constrained multi-hop wireless networks," in *Proceedings of the 3rd Annual IEEE Communications Society on Sensor and Adhoc Communications and Networks*, vol. 2, pp. 402–411, Reston, Va, USA, September 2006.
- [6] J. Polastre, J. Hill, and D. Culler, "Versatile low power media access for wireless sensor networks," in *Proceedings of the 2nd International Conference on Embedded Networked Sensor Systems (SenSys '04)*, pp. 95–107, 2004.
- [7] ANSI/IEEE Std 802.11, 2007, <http://standards.ieee.org/getieee802/download/802.11-2007.pdf>.
- [8] L. Huang and T.-H. Lai, "On the scalability of IEEE 802.11 ad hoc networks," in *Proceedings of the 3rd International Symposium on Mobile Ad Hoc Networking and Computing (MobiHoc '02)*, pp. 173–182, June 2002.
- [9] D. Zhou and T.-H. Lai, "A compatible and scalable clock synchronization protocol in IEEE 802.11 ad hoc networks," in *Proceedings of the International Conference on Parallel Processing*, pp. 295–302, 2005.
- [10] D. Zhou and T.-H. Lai, "A scalable and adaptive clock synchronization protocol for IEEE 802.11-based multihop ad hoc networks," in *Proceedings of the International Conference on Mobile Adhoc and Sensor Systems Conference*, pp. 8–17, 2005.
- [11] M. D. Lemmon, J. Ganguly, and L. Xia, "Model-based clock synchronization in networks with drifting clocks," in *Proceedings of the Pacific Rim International Symposium on Dependable Computing*, pp. 177–184, 2000.



**Hindawi**

Submit your manuscripts at  
<http://www.hindawi.com>

